



ORIGINAL RESEARCH

Boron stimulates fruit formation and reprograms developmental metabolism in sweet cherry

Michail Michailidis^{1,2} | Christos Bazakas^{1,3,4} | Marios Kollaros⁵ |
 Ioannis-Dimosthenis S. Adamakis⁶ | Ioannis Ganopoulos^{1,3} |
 Athanassios Molassiotis⁵  | Georgia Tanou^{1,2} 

¹Joint Laboratory of Horticulture, ELGO-Dimitra, Thessaloniki-Thermi, Greece

²Institute of Soil and Water Resources, ELGO-Dimitra, Thessaloniki-Thermi, Greece

³Institute of Plant Breeding and Genetic Resources, ELGO-Dimitra, Thessaloniki-Thermi, Greece

⁴Department of Comparative Development and Genetics, Max Planck Institute for Plant Breeding Research, Cologne, Germany

⁵Laboratory of Pomology, Department of Horticulture, Aristotle University of Thessaloniki, Thessaloniki-Thermi, Greece

⁶Department of Biology, National and Kapodistrian University of Athens, Athens, Greece

Correspondence

Georgia Tanou, Joint Laboratory of Horticulture, ELGO-Dimitra, Thessaloniki-Thermi 57001, Greece.
 Email: gtanou@swri.gr

Funding information

Operational Program 'Central Macedonia 2021-2027'. Grant/Award Number: KP6-0078866

Edited by Y. Jiao

Abstract

Boron modulates a wide range of plant developmental processes; however, the regulation of early fruit development by boron remains poorly defined. We report here the physiological, anatomical, metabolic, and transcriptomic impact of pre-flowering boron supply on the sweet cherry fruit set and development (S1–S5 stages). Our findings revealed that endogenous boron content increased in early growth stages (S1 and S2 stages) following preflowering boron exogenous application. Boron treatment resulted in increased fruit set (S1 and S2 stages) and mesocarp cell enlargement (S2 stage). Various sugars (e.g., fructose and glucose), alcohols (e.g., myo-inositol and maltitol), organic acids (e.g., malic acid and citric acid), amino acids (e.g., valine and serine) accumulated in response to boron application during the various developmental stages (S1–S5 stages). Transcriptomic analysis at early growth (S1 and S2 stages) identified boron-responsive genes that are mainly related to secondary metabolism, amino acid metabolism, calcium-binding, ribosome biogenesis, sugar homeostasis and especially to photosynthesis. We found various boron-induced/repressed genes, including those specifically involved in growth. Several heat shock proteins displayed distinct patterns during the initial growth in boron-exposed fruit. Gene analysis also discovered several putative candidate genes like *PavPIP5K9*, *PavWAT1*, *PavMIOX*, *PavCAD1*, *PavPAL1* and *PavSNRK2.7*, which could facilitate the investigation of the molecular rationale underlying boron function in early fruit growth. Substantial changes in the expression of numerous transcription factors, including *PavbHLH25*, *PavATHB.12L*, and *PavZAT10.1,2* were noticed in fruits exposed to boron. The current study provides a baseline of information for understanding the metabolic processes regulated by boron during sweet cherry fruit early growth and fruit development in general.

This is an open access article under the terms of the [Creative Commons Attribution-NonCommercial-NoDerivs](https://creativecommons.org/licenses/by-nc-nd/4.0/) License, which permits use and distribution in any medium, provided the original work is properly cited, the use is non-commercial and no modifications or adaptations are made.

© 2023 The Authors. *Physiologia Plantarum* published by John Wiley & Sons Ltd on behalf of Scandinavian Plant Physiology Society.

1 | INTRODUCTION

The transition of ovaries into fruit (fruit set) and fruit development are part of a genetically controlled developmental program existing in most flowering plants (Shinozaki et al., 2020). Particularly, fruit set and early growth deficits remain among the most important challenges to sustaining yields of fruit trees, including sweet cherry (Garratt et al., 2023), which is frequently characterized by low fruit set rate or premature fruitlet abscission, resulting in lower production (Sabir et al., 2021). However, our understanding of cherry fruit formation and its molecular regulation is limited, though some key physiological events are known as essential for fruit development. Initiation of fruit growth and development occurs shortly after full bloom, following fertilization and seed set (Vignati et al., 2022). The developmental growth rate of sweet cherry (drupe) can be described by a double sigmoid curve (stages I–III) (Gibeaut et al., 2017). In the initial exponential phase (stage i), the ovary either aborts or starts all the subsequent morphological changes, leading to fruit formation (Alkio et al., 2014). Stage 1, beginning at anthesis, also includes the acceleration of the growth of the ovary approximately 2 weeks before anthesis. During the preflowering period, the cells of the epidermis are already well-differentiated, with an elongated shape, and increase their size slowly (Vignati et al., 2022), indicating that some events occurring prior to anthesis may affect sweet cherry fruitlet development. Although the mechanisms influencing fruit set in sweet cherry are complex, the reduced fruit set may be associated with the genotype, self-incompatibility, stigmatic receptivity, pollen vectors such as bees, weather conditions during pollination as well as inadequate nutrient availability during critical stages of flowering (Garcia Montiel et al., 2010). Particularly, the abscission of flowers after fertilization can be mainly attributed to competition for nutrient supply among developing fruit and between fruit and actively growing shoots acting as sinks (Falchi et al., 2020).

Boron is one of the essential nutrients for the optimum growth, development, yield, and quality of crops. It performs many important functions in plants and is mainly involved in the structural integrity of the cell walls and the function of cell membranes. Boron levels are higher in floral than in vegetative tissues, suggesting a specific involvement of boron in the reproductive process (Brown et al., 2002). For example, boron could play a role in female reproductive organs and their interaction during pollen tube growth through the style and into the ovary (Fang et al., 2019). Despite these findings, there are contradictory reports concerning the effect of boron nutrition on fruit set in a variety of perennial tree crops, including sweet cherry (Wojcik et al., 2008; Wojcik & Wojcik, 2006; Ziogas et al., 2020). In addition, no information exists about the molecular events involved in these processes, which could help to better understand boron-associated fruit biology.

Boron is especially immobile in most plant tissues and does not readily move from the different parts of the tree to the buds, where it is necessary for pollen production, growth of the pollen tube, and other reproductive functions (Botelho et al., 2022). Hence, in this work, we examined the physiology of the impact of preflowering

boron application on the initial set and early fruit growth coupled with a transcriptome and metabolomic analysis using the sweet cherry as an experimental model, which yields insight into the metabolic network associated with boron nutrition in fruit biology. We summarize our findings in a model highlighting the function of boron application in regulating fruit set and early growth of sweet cherry.

2 | MATERIALS AND METHODS

2.1 | Experimental design and fruit sampling

Experiments were conducted at an experimental orchard of sweet cherry (*Prunus avium* L.) on the farm of the Aristotle University of Thessaloniki (40°32'00.4" N and 22°59'04.1" E, Central Macedonia, Northern Greece) during the 2020 growing season. The orchard consisted of 11-year-old “Skeena” sweet cherry trees, planted at 5 m × 4 m spacing between rows and along the row, grafted onto “MaxMa 14” rootstock and trained in open vases. Boron sprays were performed at the green tip stage (9 days before flowering; stage 55 based on Biologische Bundesanstalt, Bundessortenamt and Chemical Industry, BBCH scale, Figure 1A) (Fadón et al., 2015) using 0.2% (w/v) (32 mM) boric acid and 0.02% Tween 20 dissolved in distilled water. *Spray with distilled water served as the control.* The selection of boric acid dose and the time of application was based on previously published reports (Ziogas et al., 2020). The cultivar “Skeena” was chosen because it is self-fertile (Kappel et al., 2003). Three biological replicates of 15 branches harvested from 5 trees (3 branches per tree) were analyzed for boron treatment and control. In each branch, there were 9–12 rosettes and in each rosette, there were 5–8 flower buds. Sampling and analysis of various physiological traits of fruit were conducted at 12d (stage 1, S1), 23d (stage 2, S2), 37d (Stage 3, S3), 46d (stage 4, S4), and 63d (stage 5, S5; commercial harvest) days (d) after full blossom (DAFB). Just after harvest, samples were immediately immersed in liquid nitrogen and stored at –80°C for further analysis.

In a second experiment conducted the following year (2021), the cultivars “Paulus” (self-fertile) and “Aida” (cross-fertile) (Schuster, 2017) were also treated with boric acid (0.2%, w/v, 32 mM) as described above and their fruit set along with cell width and height were determined.

2.2 | Fruit set, boron concentration, and physiological traits

Fruit set evaluation was performed in five branches per tree ($n = 15$) during full blossom and at 26 DAFB (fruit retention stage). In detail, the number of flowers in each branch and the number of fruit at 26 DAFB were measured, then the percentage of fruit set was calculated through the equation: $\text{Fruit set} = (\text{No. of fruit} \times \text{No. of flower}^{-1}) \times 100$. Boron concentration was determined in 3 batches of 15 fruits (exo-mesocarp tissue, $n = 3$) for each treatment/stage.

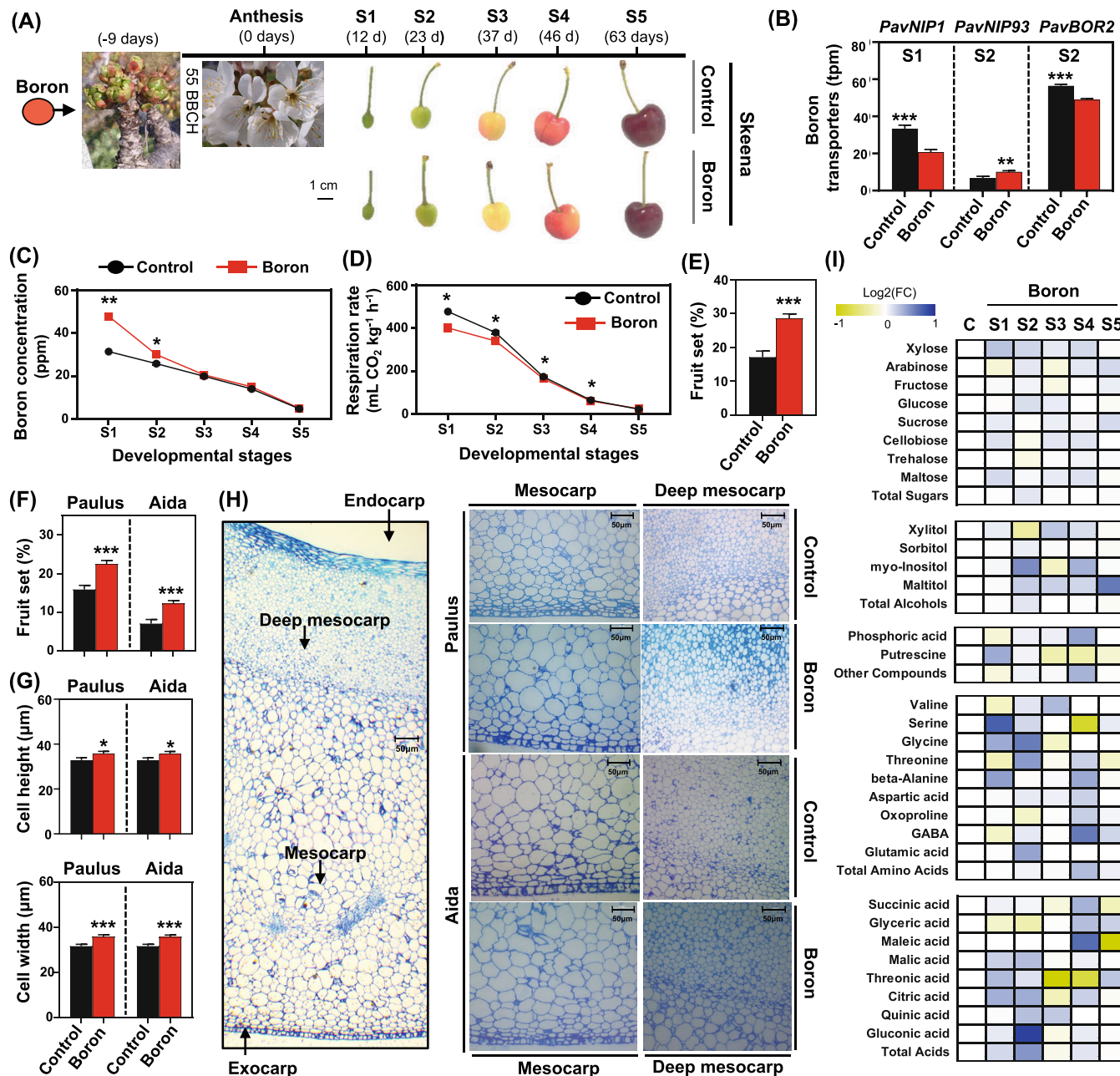


FIGURE 1 Phenotypical, physiological and anatomical features of sweet cherry fruit exposed to boron. (A) Graphic illustration of the experimental design; boron treatment was performed at the green tip stage (9 days before flowering, stage 55 based on Biologische Bundesanstalt, Bundessortenamt and Chemical Industry, BBCH scale) in “Skeena” trees using boric acid. Sampling and analysis of fruit were conducted at 12d (stage 1, S1), 23d (stage 2, S2), 37d (Stage 3, S3), 46d (stage 4, S4), and 63d (stage 5, S5; commercial harvest) days (d) after full blossom (DAFB). Boron application was also performed in the “Paulus” and “Aida” trees (F) as described above (A). (B) Expression of boron transporters genes (tpm) at S1 and S2 stages in “Skeena” fruit. (C) Boron concentration in cherry fruit (exo- and meso-carp tissues) and (D) fruit respiration rate during fruit development (S1-S5 stages) in “Skeena”. Fruit set (E) in “Skeena” and (F) in “Paulus”, and “Aida” cultivars at 26 days after full blossom (DAFB). (G) Cell width and height, and (H) microscope observations in boron-treated “Paulus” and “Aida” fruit at 26 days after full blossom. Additional physiological data are provided in Table S1. Each point/bar represents the mean of at least three biological replicates (each biological replicate consists of 15 fruits or 5 branches) and vertical lines represent the standard error of the mean (SEM). Differences were detected based on the Student *t*-test; **p* ≤ 0.05, ***p* ≤ 0.01, ****p* ≤ 0.001. Scale bars: as depicted on the image. Primary metabolite analysis in response to boron treatment in exo- and meso-carp tissues across the various developmental stages of “Skeena” fruit. (I) Heatmap depicts the difference in metabolite relative abundance between control and boron treatment. Each cell represents the log₂(FC) (blue indicates an increase and yellow indicate a decrease of metabolites in response to boron treatment). Metabolite data are provided in Table S2.

Samples were dried (72°C for 48 h), ground into a fine powder and incinerated in a muffle furnace (550°C for 5 h); the ash was then dissolved in 2N HCl. The concentration of boron was measured by the azomethine-H method (Sotiropoulos et al., 2006). Fruit physiological traits, including fresh and dry weight, color indexes (L^* , a^* , and b^*), and textural property (the required force to achieve 10% deformation in $N\text{ mm}^{-1}$) have been analyzed (Table S1) as described in detail by Michailidis et al. (2021). Yield (tons per hectare) was also calculated. The respiration rate of fruit was measured in three biological batches of 15 fruits that were enclosed in 2-L air-tight jars for 30 min at 20°C using a gas chromatograph and TCD detector (GC-2014ATF Shimadzu).

2.3 | Microscopy observations

Tissue samples excised from the median part of two “Paulus” and “Aida” fruits at 26 DAA going from exocarp to endocarp were subjected to chemical fixation, dehydration and embedding in White acrylic resin (LRW) as previously described by Pappas et al. (2022). Transverse sections of specimens embedded in LRW were taken with an Ultratome III Type 8801A (LKB), transferred on glass slides and stained with 0.5% (w/v) toluidine blue O.

Six transverse sections of exo- and mesocarp were performed in three biological replicates. Cell width and height were determined in 50 cells per section from both mesocarp and deep mesocarp of fruit using a microscope (Axio Imager M.2 Zeiss) coupled with a camera (Axiocam 305 color) and analyzed using ZEN software 3.6 according to the manufacturer's instructions.

2.4 | Primary metabolites analysis

Primary polar metabolites were determined following a well-established protocol (Lisec et al., 2006). In 2-mL screw cap vials, frozen lyophilized exo- and meso-carp tissue (0.5 g) was added along with methanol (1.4 mL) and adonitol (0.1 mL; 1 mg mL^{-1}) and incubated (10 min at 70°C). The supernatant was collected (after centrifugation; 11,000g, 4°C, 10 min), and chloroform (0.75 mL) as well as dH_2O (1.5 mL) were added. Next, the upper phase (0.15 mL; after centrifugation; 2200g, 4°C, 10 min) was transferred into a 2 mL vial glass and placed to dry under vacuum (2 days). Finally, methoxyamine hydrochloride (40 μL of 20 mg mL^{-1}) was added and incubated for 120 min at 37°C, then MSTFA reagent (70 μL of *N*-methyl-*N*-trimethylsilyl-trifluoroacetamide) were added, incubated for 30 min at 37°C and transferred into 2 mL vial glass with insert. Analysis was performed using a PerkinElmer Clarus® 590 GC equipped with Clarus® SQ 8 S MS (USA) and chromatogram visualization and analysis were performed using TurboMass™ software as described by Polychroniadou et al. (2022). Standard compounds and database NIST11 of unknown peaks were used for the determination of polar metabolites. The primary polar metabolites were expressed as the relative abundance of the adonitol. The relative abundance of metabolites is provided in Table S2.

2.5 | Library construction and RNA-seq analysis

Total RNA was extracted using Monarch Total RNA Miniprep Kit (New England BioLabs Inc.) from control and boron treatment cherries at developmental stages S1 and S2 in three biological replicates (Michailidis et al., 2020). Poly-A enriched libraries were prepared with Illumina® Truseq stranded RNA Library Prep Kit following manufacturer's instructions. Quality control of libraries (quantification and qualification of each library) were performed using an Agilent 5300 Fragment Analyzer. Each library was sequenced on an Illumina® Novaseq 6000 platform.

Low quality reads ($Q > 28$) and unknown sequences (N) were trimmed and filtered with Trim Galore. Thereafter, reads aligned against *Prunus avium* L. cv. “Tieton” reference genome (Wang et al., 2020) with Hisat2 with default parameters and then data analysis was performed as previously described (Polychroniadou et al., 2022). Genes with q -value (p -value adjusted) below 0.01 were included in the differentially expressed genes (DEGs) without any other threshold (Tables S3–S5).

2.6 | Real-time reverse transcription-PCR analysis

Total RNA (10 μL), which has been isolated for RNAseq analysis, was used for validation with qRT-PCR experiment. cDNA construction was reverse-transcribed from 10 ng RNA using LunaScript® RT SuperMix Kit (New England Biolabs Inc.). Real-time PCR was performed using 2 μL cDNA, 0.5 μL for forward and reverse primers and following the instruction of Luna® Universal qPCR Master Mix (New England Biolabs Inc.) in a QuantStudio® 5 Real-Time PCR System (96-well, Thermo Fisher Scientific). Primers were designed with Primer3Plus (<http://www.bioinformatics.org/cgi-bin/prime3plus/>) (Table S6). The qPCR program was performed as described by Tanou et al. (2015). Ct recorded at 0.2 ΔRn and melt curve constructed to verify PCR products. Data were analyzed using the $\Delta\Delta\text{Ct}$ method (Livak & Schmittgen, 2001).

2.7 | Weighted gene co-expression network analysis

Weighted gene co-expression network analysis (WGCNA) was performed on the RNAseq of DEGs (q value < 0.01) and metabolome datasets between boron treatment and control samples in both stages (S1 and S2), using the R package (Langfelder & Horvath, 2008). The WGCNA workflow has been previously described in detail (Polychroniadou et al., 2022). The co-expression network was constructed based on the weighted edges with weighted value ≥ 0.5 and visualized by using Cytoscape (v.3.9.1) (Shannon et al., 2003).

2.8 | Statistical analysis and data processing

One-way analysis of variance (ANOVA) was conducted using SPSS v27.0. Mean values of ripening traits, boron concentration,

metabolites and gene expressions (from qRT-PCR) were compared by *t*-test ($p \leq 0.05$). Gene ontology (GO) and protein enrichment analysis was employed using PANTHER software (Thomas et al., 2022). Transcription factors annotation was performed in *Arabidopsis thaliana* homologs using the AtTFDB database (Yilmaz et al., 2011). Metabolites and transcripts (using *Arabidopsis thaliana* homologs) were mapped to the KEGG database (Ogata et al., 1999). The association between RNA-seq data and qRT-PCR Ct values was assessed by the Pearson correlation coefficient.

3 | RESULTS

3.1 | Exogenously applied boron increased internal boron concentration and fruit set

In response to external boron application at the preflowering stage (Figure 1A), the expression of genes related to boron transportation (*PavBOR2* and *PavNIP93*) decreased at S1 and S2 respectively, whereas *PavNIP1* increased at S2 (Figure 1B). Meanwhile, the endogenous boron concentration was increased in “Skeena” fruit at S1 and S2 stages but remained unaffected in the other stages (S3–S5) (Figure 1C). Boron treatment reduced the respiration activity of fruit from S1 to S4 stages (Figure 1D). Fresh weight at S1, as well as yield at harvest, was increased in boron-treated cherries while other fruit characteristics, including dried weight, deformation force and color were not affected by boron (see Figure S1 and Table S1). Interestingly, boron application increased the fruit set of the self-fertile “Skeena” cultivar (Figure 1E). To further characterize the impact of boron in the sweet cherry fruit set, we also performed the same boron treatment in the subsequent year using one self-fertile (“Paulus”) and a cross-fertile (“Aida”) cultivar. This follow-up experiment indicated that boron also increased the fruit set in both “Paulus” and “Aida” cultivars (Figure 1F). In addition, microscope observations of “Paulus” and “Aida” fruit sections at 26 DAFB revealed cell enlargement upon boron application as documented by the higher cell width and height in boron-treated fruit (Figure 1G,H).

3.2 | Changes in primary metabolism of cherry fruit following boron treatment

Thirty-one primary metabolites were quantified at various stages (S1–S5), which were divided into five categories, including sugars (eight), alcohols (four), acids (eight), amino acids (nine), and other substances (two) (see Table S2). Based on the relative abundance of metabolites data from all stages, the constructed PCAs revealed a split between S1 and S2 only when separating S1 and S2 stages from the remaining stages (57.4% of variance), and a clear separation among all fruit stages regardless of boron treatment (Figure S2A,B). In detail, the first PCA model explained 78.6% of the overall variance (Figure S2A), while the second PCA model explained 61.5% of the overall variance, with PC1 relating to stages (45.9% of variation) and PC2 relating to treatments (15.6% of variance) (Figure S2B).

Boron treatment raised the total acids at S2 and S4, total sugars at S2, and total amino acids at S4 (Figure 1I). In general, we observed that several metabolites increased during fruit growth by boron. Particularly, two sugars (fructose; S5, glucose; S2), two alcohols (myo-inositol; S4, maltitol; S4 and S5) five organic acids (succinic acid; S4, maleic acid; S3 and S4, malic acid; S2, citric acid; S1, gluconic acid; S2), four amino acids (valine; S4, serine; S1, beta-alanine; S1, GABA; S4), and one other compound (phosphoric acid; S4) were increased in response to boron. Threonic acid (acid) was initially increased at S1 and then decreased at the S3 stage in boron-treated cherries (Figure 1I).

3.3 | The boron-related gene expression profile in developing sweet cherry fruit

Since an accumulation of boron was observed at S1 and S2 (Figure 1A), we conducted RNA-seq analysis in untreated (control) and boron-treated fruit in these stages to identify boron-affected genes (Figure 2). Transcriptomic data analysis revealed a clear distinction between stages and a distinguishable separation between control and boron-treated samples (Figure S3A). The comparative expression analysis between control and boron supplementation identified a total of 407 (102 upregulated) and 998 (549 upregulated) differentially expressed genes (DEGs) at stages S1 and S2, respectively (Figure S3B). In response to boron, five genes were found to be upregulated in both stages (S1 and S2), whereas 27 genes were downregulated in both stages (Figure 2A). Common upstream genes include beta-amylase 9 (*PavBAM9*) and phosphatidylinositol 4-phosphate 5-kinase 9 (*PavPIP5K9*), whereas common downstream genes consist of eight enzymes (*PavAPR3*, *PavCYP.82G1L*, *PavCSE.1*, *PavPAP.17*, *PavPP2C.51*, *PavLTICP*, *PavSAMDC*, *PavSGR*) and two transcription factors (TFs; *PavMYB44L*, *PavATHB.12 L*) (Figure 2B). To further investigate boron-responsive transcriptome changes, 10 highly expressed genes (up- and downregulated) at each developmental stage are identified (Figure 2C, see also Table S3). In the S1 stage, boron-associated significantly upregulated DEGs include *PavADH*, *PavGDH1* and *PavbHLH25* (TFs), whereas the S2 stage involves *PavEP3.2*, *PavBAS*, *PavAO*. The group of DEGs that are downregulated by boron at the S2 stage involves three genes (*PavNIR1*, *PavNUDT18*, and *PavHIBYL-CoA1*) and four TFs (*PavERF109*, *PavbHLH25*, *PavTTL*, and *PavGLABRA2*) (Figure 2C, see also Table S3). To further validate the RNA-seq data, five DEGs were investigated by qRT-PCR. The Pearson coefficient between qRT-PCR data and transcriptome profiles was very high ($R^2 = 0.90$), indicating that the RNA-seq results were credible (see Figure S4 and Table S4).

3.4 | Gene ontology and pathway classifications of boron-responsive genes

To obtain a better understanding of the identified DEGs, an analysis based on *Arabidopsis thaliana* homologs via gene ontology (GO), protein class and KEGG pathway classifications were employed (Figure 2; see Figure S5 and Table S5). To generate boron-responsive gene

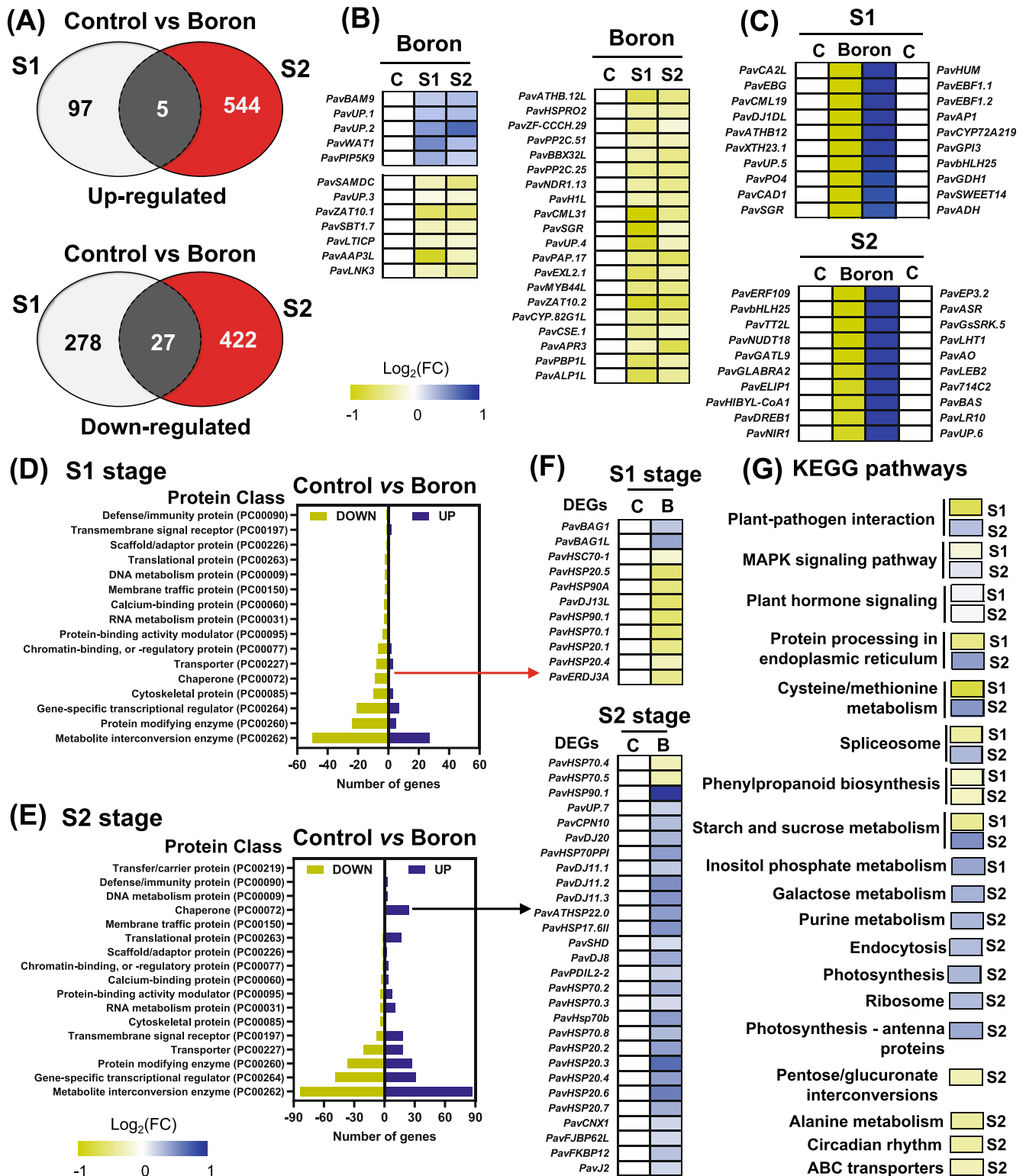


FIGURE 2 Differentially expressed genes (DEGs) of boron treatment at S1 and S2 developmental stages of “Skeena” fruit. (A) Venn diagram showing the up- and downregulated DEGs in S1 and S2 stages after the boron treatment. (B) Heatmap illustrated the commonly affected (up- and downregulated) DEGs in response to boron treatment in both stages. (C) Heatmap with highly expressed (up-/downregulated) DEGs separately in S1 and S2 stages. Class of DEGs that changed (upregulated or downregulated) in boron-treated fruit at (D) S1 and (E) S2 stages. (F) Heatmap of chaperones that changed (upregulated or downregulated) in boron-treated cherries at S1 and S2 stages. (G) KEGG pathway analysis regarding the calculation of the average fold-change of DEGs that participate in each pathway. Heatmaps and bars of class indicate yellow color for the decrease and blue for the increase of DEGs following boron treatment. Transcriptomic data, KEGG pathways and abbreviations are provided in Tables S5 and S3.

clustering, a categorization of DEGs concerning GOs and especially their biological process, molecular function and cellular component was performed (Figure S5A,B). In relation to the gene's biological process, most of the boron-responsive genes in both stages were associated with cellular and metabolic processes (25 genes upregulated (U)/77 genes downregulated (D), 18U/51D at S1; 138U/94D, 104U/73D at S2, respectively). In both stages, the downregulated DEGs encode proteins that participate in the reproductive process. In boron-exposed cherries, the genes annotated as a response to stimulus and transcription regulator activity were suppressed at S1 (80% D, 83% D) and induced at S2 (70% U, 63% U), whereas genes associated with transporter activity were induced at S1 (71% U) but were suppressed at S2 (62% D) and genes that participate in signaling declined in S1 (80% D) (Figure S5A,B). Boron altered several genes encoding binding proteins (10U/53D genes in S1, 73U/40D genes in S2) and catalytic activity (25U/51D genes in S1, 98U/86D genes in S2). Meanwhile, in the GO cellular component, numerous genes encoding enzymes associated with cellular anatomical entities were mainly downregulated at S1 (75% D) while slightly increasing at S2 (55% U) after boron application (Figure S5A,B).

We further identified protein class categories that were highly represented in DEGs at both stages. The majority of these DEGs belong to protein classes, such as metabolite interconversion enzyme (27U/50D genes in S1, 84U/87D genes in S2) and protein modifying enzyme (5U/24D genes in S1, 27U/37D genes in S2). Several boron-affected genes involved in transmembrane signal receptors (69% U) were exclusively detected in S2. The current transcriptomic analysis also revealed diverse changes in boron-responsive gene expression pathways between the examined stages. For example, DEGs associated with chaperones and translational proteins were suppressed at S1 (81% D and 100% D) and were induced at S2 (93% U and 89% U) (Figure 2D,E). Meanwhile, nine chaperones DEGs were downregulated (i.e., *PavHSC70-1*, *PavHSP20.5*, *PavHSP90A*), whereas two were upregulated (*PavBAG1*, *PavBAG1L*) in boron-treated fruit at S1. In contrast, 26 DEGs, most of them including heat shock proteins (i.e., *PavHSP90.1*, *PavHSP70.1-3*, *PavHSP20.6-7*), were upregulated in boron-exposed cherries, whereas two were downregulated (*PavHSP70.4-5*) at S2 stage (Figure 2F, see also Table S5).

The results also showed that five pathways, namely plant-pathogen interaction, protein processing in the endoplasmic reticulum, cysteine and methionine metabolism, spliceosome, and starch/sucrose metabolism, were deactivated by boron at S1 and then activated at S2 (Figure 2G). In contrast, pentose and glucuronate interconversions, beta-alanine metabolism, circadian rhythm, and ABC transporters were suppressed by boron at the S2 stage. The phenylpropanoid biosynthesis pathway was the only one that was depressed in boron-exposed cherries at both stages (Figure 2G).

3.5 | Differentially expressed transcription factors following boron application in sweet cherries

The functional annotation of the sweet cherry genome (Tieton Genome v2.0 Assembly & Annotation) and particularly *Arabidopsis*

thaliana homologs (AtTFDB database) were used to identify TFs that were modulated by boron at each stage. The expression of 48 and 108 TFs at S1 and S2, respectively, was significantly altered by boron treatment (Figure 3). Specifically, the boron application resulted in the upregulation of 8 and 36 TFs at S1 and S2, respectively, while 34, 66, and 6 TFs were downregulated on S1, S2, and both stages, respectively (Figure 3).

According to AtTFDB database, all the identified TFs were mainly grouped in 11 families, namely AP2-EREBP, bHLH, Homeobox, C2C2-Dof, HSF, MYB, NAC, C2C2-CO-like, GRAS, ARF, WRKY and other TFs (Figure 3). The upregulated TFs in both stages belong to bHLH (e.g., *PavIBH1.1*, *PavIBH1L*) followed by WRKY (e.g., *PavWRKY17*, *PavWRKY46*). By contrast, the TFs that belong to AP2-EREBP group (e.g., *PavERF1A*, *PavERF1B*), MYB (e.g., *PavMYB5L*, *PavMYB8L*), Homeobox (e.g., *PavATHB6*, *PavATHB14*), and NAC (e.g., *PavNAC72*, *PavNAC90*) families were downregulated by boron at both stages (Figure 3). Furthermore, WRKY (e.g., *PavWRKY40*, *PavWRKY70*) and HSF (e.g., *PavHSFB-1*, *PavHSFB-2b*) TF families were downregulated by boron at S1 only, whereas four TF families were downregulated by boron at S2 only, including ARF (e.g., *PavERF2B*, *PavERF6*), bHLH (e.g., *PavbHLH25*, *PavbHLH30*), GRAS (e.g., *PavSCR9*, *PavSCR15*), and C2C2-CO-like (e.g., *PavZFB5L*, *PavBZFB19L*) (Figure 3). Notably six TFs, specifically *PavMYB44L* (MYB), *PavATHB.12L* (Homeobox), *PavBBX32L* (C2C2-CO-like), *PavZAT10.1-2* (C2H2), and *PavUP.3* (C3H), were downregulated in both stages by boron (Figure 3).

3.6 | Expression network of boron-responsive genes and metabolites

To explore the possible transcriptome-metabolome networks related to boron, a weighted gene co-expression network analysis (WGCNA) was carried out at both stages using the normalized expression values (TPM) of DEGs and relative abundance of metabolites. For module construction, the dynamic tree cut method was used and revealed eight modules (ME), viz. blue, turquoise, yellow, green, brown, pink, black and red (Figure 4A). Among them, the turquoise module included the highest number of genes and metabolites (399), followed by blue (187) and brown (185) modules (see Table S6). Modules construction exhibited a higher association with the stages instead of boron treatment (Figure 4B). Genes from blue, turquoise, yellow, brown and black modules (ME) were downregulated, whereas genes from green, pink, and red MEs were upregulated at S1 compared to S2 (Figure 4B). Modules of blue, green, pink and red had zero interactions based on a weighted threshold above 0.5, while yellow had only two interactions. Black, brown, and especially turquoise modules exhibited many interactions (296, 513 and 21,014, respectively) (Figure 4C).

The black module consists of 46 annotated genes and two metabolites (citric acid and sucrose; see Table S6) related to two and seven DEGs, respectively (Figure 4C). In particular, citric acid is associated with *PavERF105L* (TF) and *F-box protein SKP2A-like* (FUN_027663), while sucrose is related to *PavU.P.LOC110770215* (FUN_016586), *G-type*

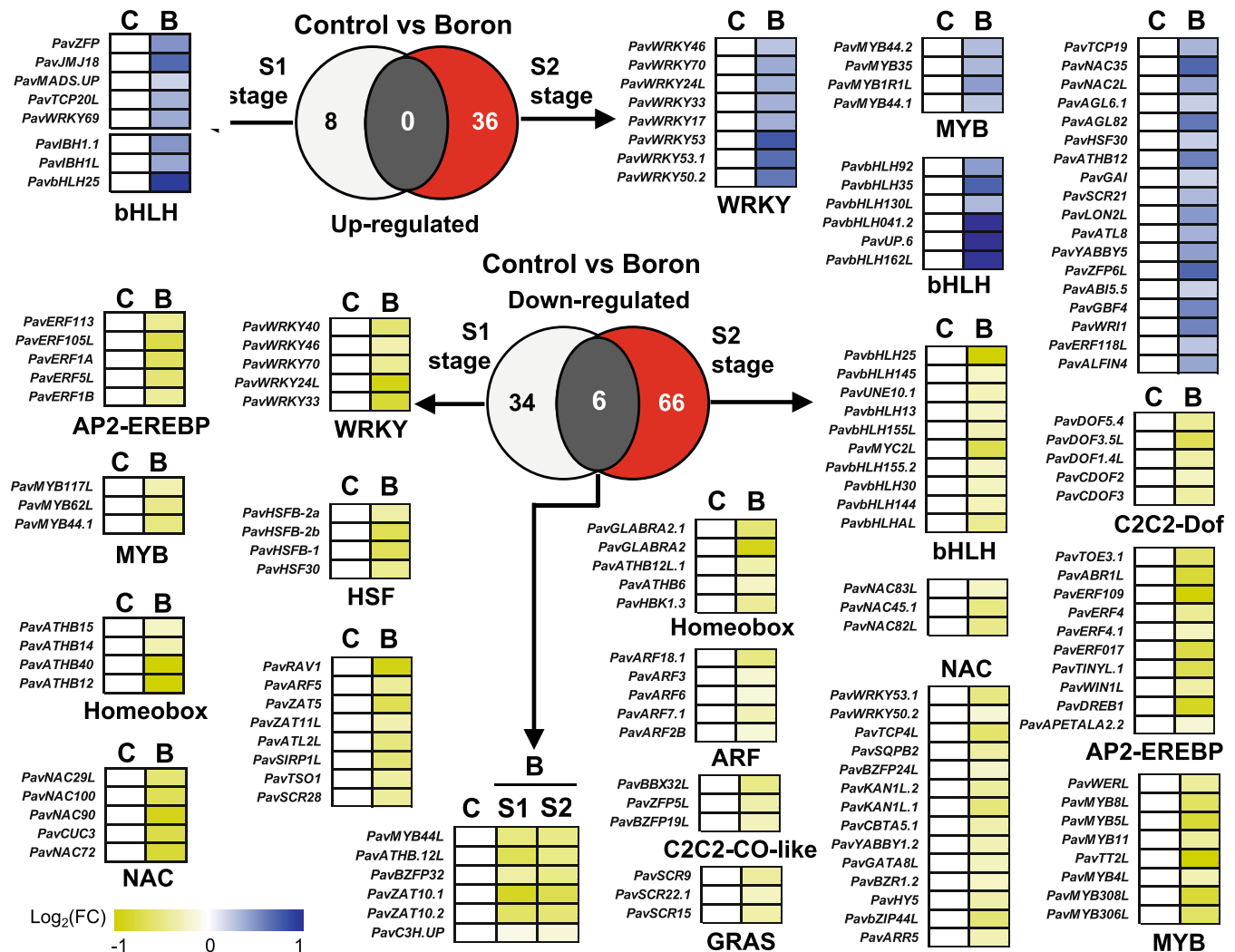


FIGURE 3 Transcription factors (TFs) analysis in boron-exposed “Skeena” fruit (control vs. boron treatment) at S1 and S2 stages based on *Arabidopsis thaliana* homologs. Venn diagrams indicating the number of boron-affected TFs at both stages. Heatmap presents the differentially expressed (up- and/or downregulated) boron-affected TFs; yellow color indicates a downregulation and blue an upregulation. Transcription factor data and abbreviations are provided in Table S3.

lectin *S*-receptor-like serine/threonine-protein kinase At1g61490 (FUN_031851), probable pectate lyase 8 (FUN_000650), PREDICTED: GDSL esterase/lipase At5g45670-like (FUN_032346), PavIAA9 (FUN_007191). Brown ME consists of 117 annotated genes and one metabolite (maltitol; see Table S6) that connected with *L*-ascorbate peroxidase 2 (FUN_021735) and *L*-cysteine desulphydrase (FUN_022504) (Figure 4C).

3.7 | Boron-affected genes related to metabolic function

To further study the metabolic function of boron, we investigated boron-related pathways at S1 and S2 stages. Several DEGs associated with starch/sucrose, cysteine/methionine metabolism and phenylpropanoid biosynthesis were increased, whereas DEGs involved in inositol and phosphate metabolism were depressed by boron at the S1 stage

(Figure 5). In detail, several DEGs involved in inositol and phosphate metabolism were upregulated (i.e., *PavPIP5K9*, *PavMIOX*), whereas most of the sugar (i.e., *PavBGLU17*, *PavGH9B1*) and amino acid (*PavHMT3*, *PavNAS*) genes were downregulated by boron (Figure 5). Phenylpropanoid biosynthesis genes (*PavCSE.1*, *PavCAD9*, *PavCAD1*) were downregulated except for genes linked to lignin biosynthesis (*PavPRX.1–2*, *PavPRX52*), which were upregulated (Figure 5).

A total of 13 KEGG pathways, including amino acids and sugars metabolism, enzyme/protein protection, were affected by boron at the S2 stage (Figure 6). Genes that participate in galactose, starch, sucrose, cysteine and methionine metabolism were upregulated at S2, even though six of them (*PavUGE1*, *PavSIP1.1*, *PavTPS9.1*, *2*, *PavHMT3*, *PavMGL*) were decreased at S1 stage (Figure 6). Five purine metabolism-related genes (*PavTIM*, *PavAGK2*, *PavRNR1*, *PavADSS*, *PavFAC1*) were increased in cherries exposed to boron. Additionally, various heat shock proteins (e.g., *PavHSP90.1*, *PavHSP70.1,2,3*, *PavHSP20.1,2,3,4,5,6,7*) were downregulated at S1 but upregulated at

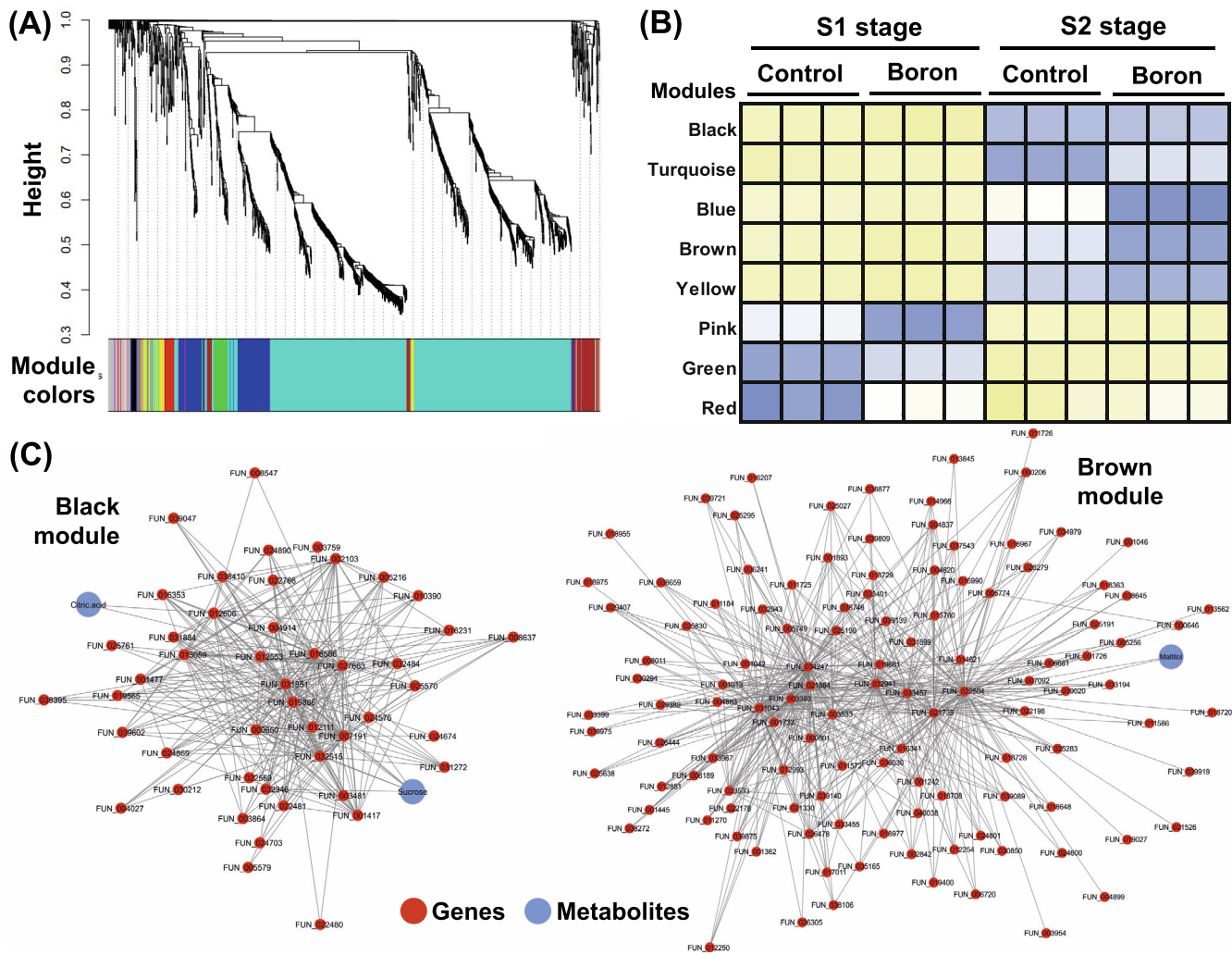


FIGURE 4 WGCNA co-expression network of DEGs and metabolites in boron-treated “Skeena” cherries at S1 and S2 stages. (A) Hierarchical cluster tree showing transcripts and/or metabolites with high co-expression level (correlation ≥ 0.9) and depict branches of the dendrogram and constitute modules labeled with different colors. (B) Heatmap of eight modules (rows) and 12 biological samples (columns), where yellow represents negative correlation and blue positive correlation. (C) Network regulations in black and brown modules presenting the gene and metabolite weighted edges (weighted value ≥ 0.5). Visualization of regulation networks was conducted using Cytoscape software. The orange-red circle represents the gene and the blue the metabolites.

S2. Genes related to photosynthesis, antenna proteins (e.g., *PavPSBQ-2*, *PavLHCA1*, 2, 3, 4, *PavLHCB2.1*, 4.2, 5) and ribosome biogenesis (e.g., *PavRPS3Ae*, *PavRPL2*, *PavSH3*) were increased by boron at S2 stage (Figure 6).

The significant role of boron in sweet cherry metabolism is also demonstrated through the upregulation of several genes involved in MAPK and plant hormone signaling at S2 (Figure 6). These genes may regulate important processes, such as stress adaptation and stomata closure through abscisic acid (*PavPYL4*, *PavRCAR1*, *PavABF2*, *PavbZIP*), fruit ripening via ethylene (*PavETR2*, *PavHCHIB*), cell enlargement through auxin pathway (*PavIAA9*, 11, 18) and stem growth via gibberellin (*PavRGL2*). Boron nutrition is also characterized by plant-pathogen leading to cell hypersensitive response and programmed cell death (PCD) through activation of various genes, among them kinases (*PavCPK2*, *PavCDPK19*), calmodulin (*PavMSS3*, *PavEFCBP*), cyclic

nucleotide-gated ion channel (*PavCNGC1*, 4) and respiratory burst oxidase (*PavRBOHD*) (Figure 6). Many DEGs that related to cell wall metabolism, such as pectinesterase inhibitor and pectin lyase (*PavP-MeI.1*, *PavPMEi.2*, *PavPEL*) were decreased at S2. Finally, genes associated with circadian rhythm (*PavPRR5*, *PavHY5*, *PavHY5-like.2*) and ABC transporters (*PavABC1*, *PavABC11*, *PavABCG22*) were inhibited in boron-treated cherries at S2 (Figure 6).

4 | DISCUSSION

Fruit set is the developmental transition from the ovary to young fruit, following pollination and fertilization (Vignati et al., 2022). Results regarding the impact of boron in fruit sets are often contradictory (Wojcik et al., 2008; Wojcik & Wojcik, 2006; Ziogas et al., 2020) while

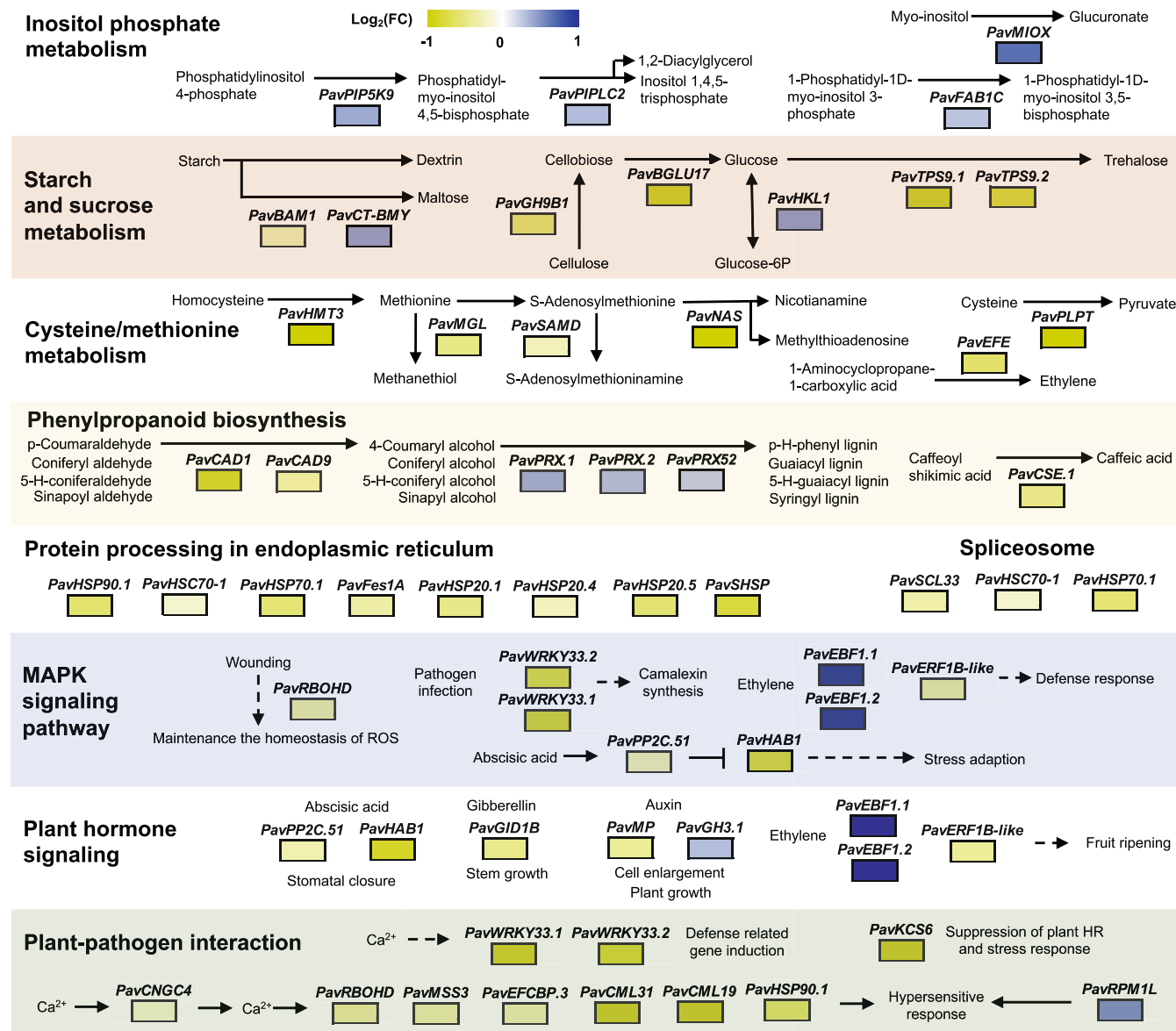


FIGURE 5 Specific pathways of sweet cherry genes (based on *Arabidopsis thaliana* homologs) de- or co-activated by boron treatment at the S1 stage. A yellow cell indicates an upstream fold change and a blue cell indicates a downstream fold change in gene expression. Transcripts and abbreviations are provided in Tables S3 and S5.

no information exists about the molecular responses of young fruit to boron feeding. As fruit set is tightly linked to yields (Garratt et al., 2023), understanding the mechanisms of how fruitlets respond to preflowering boron application is of considerable economic and scientific interest. In the current study, using the sweet cherry fruit as a model, we conduct a comprehensive analysis to characterize the molecular framework of boron-mediated fruit set and early fruit development.

4.1 | Boron enhances fruit set and provokes cell enlargement

Although boron in most plant species has low mobility in the phloem, it forms complexes in species-rich sorbitol and fructose in *Prunus*,

allowing it to move through the phloem, thereby making it a highly mobile element (Hu et al., 1997). In this regard, the observed increase of boron content in boron-treated cherries at the S1 and S2 stages and the subsequent reduction to the control level after the S3 stage (Figure 1A) might be related to the boron's mobility to other tissues (i.e., leaves, shoots) via the phloem. Our data indicate that boron enhanced the fruit set, possibly by improving the fertilization process and subsequent plant source-sink relations. Given that self-pollen tubes often grow more slowly than cross-pollen tubes (Sedgley & Griffin, 1989) and hence may take longer to reach the ovule, it is possible that boron improves fruit set following self-pollination in “Skeena” and “Paulus” cultivars by accelerating pollen germination and pollen tube growth, resulting in fruit formation. Boron was linked to source-sink development of branches in

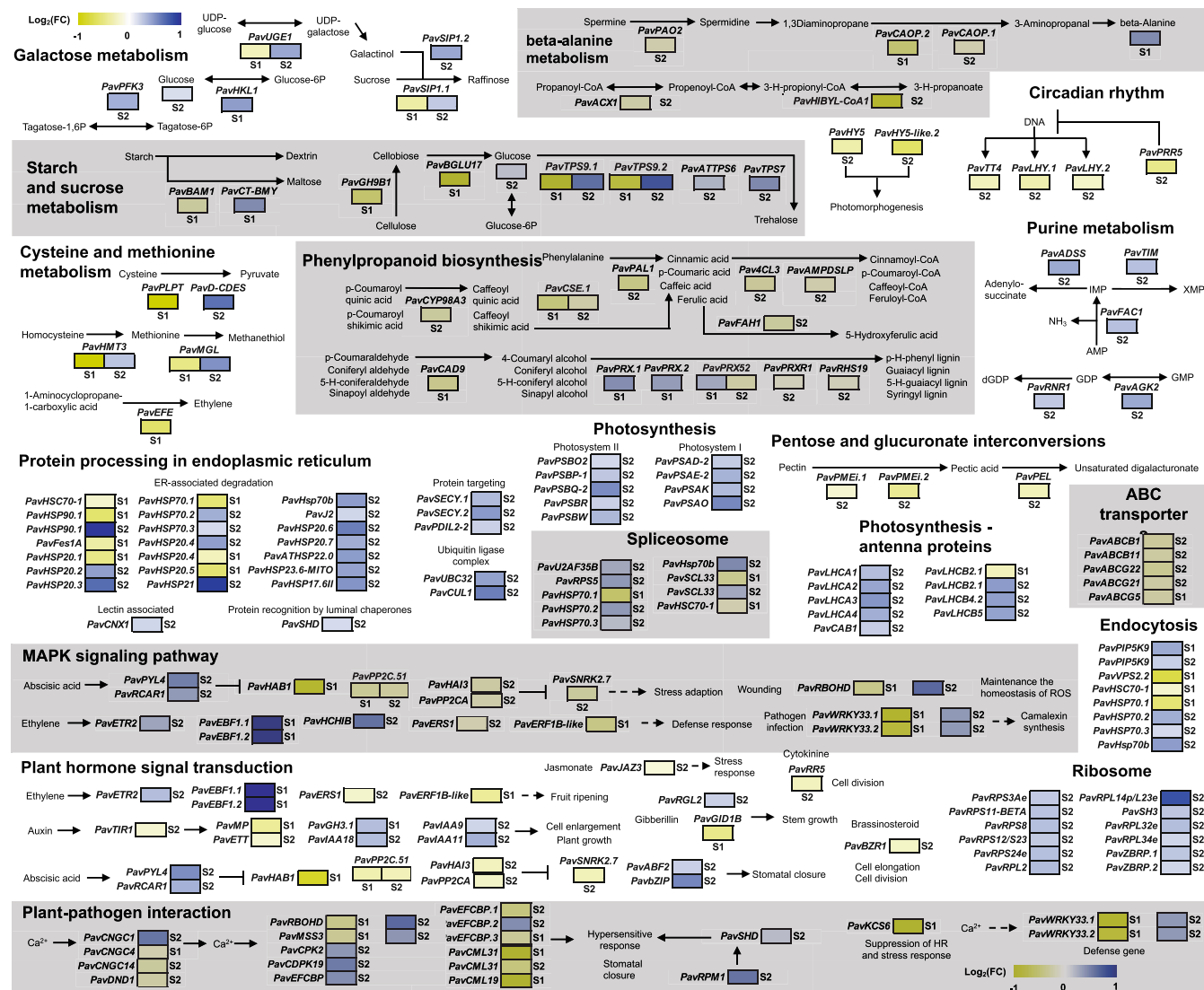


FIGURE 6 Specific pathways of sweet cherry genes (based on *Arabidopsis thaliana* homologs) de- or co-activated by boron at the S2 stage and the corresponding de- or co-activation in the S1 stage. A yellow cell indicates an upstream fold change and a blue cell indicates a downstream fold change of gene expression and/or metabolic abundance. Transcripts, metabolites and abbreviations are provided in Tables S2, S3 and S5.

soybeans (Schon & Blevins, 1990) but their role in source-sink relations in fruit remains to be established.

Apart from evidence showing a boron-related regulation of fruit set, we found greater cell enlargement in boron-treated cherries (Figure 1G,H). This cell enlargement could be explained by the activation, at S2 stage, of various genes involved in growth regulation by gibberellin via DELLA protein (e.g., *PavRGL2*) and by auxin (e.g., *PavIAA9*, 11, 18). There is evidence that growth regulators, such as GA₄ and auxin, have a crucial role in early sweet cherry fruit development and cell enlargement (Terbia et al., 2016). Since boron increased the level of several metabolites such as glucose, gluconic acid, threonic acid, citric acid, malic acid, serine, and beta-alanine during stages S1 and S2 (Figure 1I), we also hypothesized that the activation of primary metabolism could affect cherry growth. Such changes in primary metabolism may provide energy and biosynthetic precursors to support fruit growth (Beauvoit et al., 2018; Goulas et al., 2015) or/and contribute to a

lignified endocarp (Canton et al., 2020). It was previously shown that most of the cell volume in fleshy fruit is occupied by a large central vacuole that participates in fruit growth via its enlargement driven by the accumulation of osmolytes, such as organic acids and sugars, through activation of the primary metabolism (Beauvoit et al., 2018). In support of this, we found that the early fruit boron loading (Figure 1A) was accompanied by an increase in fruit respiration rate during development (Figure 1C), which in turn may be linked to both increased fruit set and enhanced metabolic activity at various ovary post-fertilization stages (Figure 6).

4.2 | Boron specifically reprograms sweet cherry transcriptome at the early stages of development

As this was the first study to characterize the boron-responsive transcriptome changes in fruit, current data provide new insights into

gene expression in the context of boron feeding in developmental fruit biology. Particularly, this study identified five genes, namely inactive β -amylase 9 (*PavBAM9*), phosphatidylinositol 4-phosphate 5-kinase 9 (*PavPIP5K9*), WAT1-related protein (*PavWAT1*), and two unknown function proteins (*PavUP.1*, *.2*) (Figure 2) that were upregulated by boron at both developmental stages (S1 and S2). β -Amylases (BAMs) are key enzymes of transitory starch degradation in chloroplasts, a process that buffers the availability of photosynthetically fixed carbon to maintain energy levels and plant growth (David et al., 2022). Cherry fruit is green at the early stages of development and contains the necessary pigments to carry out photosynthesis (Vignati et al., 2022), suggesting that fruitlet photosynthesis can contribute to their gain in biomass. This led to the hypothesis that *PavBAM9* may function as a regulator of starch degradation that influences the cell enlargement of fruit exposed to boron, although no mechanism has yet been elucidated. Furthermore, cell expansion also involves cytoskeleton reorganization and the reorientation of each of the cell wall's components (Carpita & Gibeaut, 1993). Thus, the activation of *PavPIP5K9* following boron application (Figure 2) could be linked with the increased cell expansion (Figure 1G,H) because it was suggested that PIP5K9 regulates developmental processes through cytoskeleton dynamics in *Arabidopsis* (Lou et al., 2007). Our analysis further showed that *PavWAT1*, a gene required for secondary cell-wall deposition (Ranocha et al., 2013), was upregulated in boron-treated fruits (Figure 1A), proposing that this gene may control the cell wall formation, which constitutes the bulk of fruit biomass (Zhong & Ye, 2015).

Apart from evidence showing a common boron-driven upregulation of the transcriptome, we found significantly lower expression of 27 genes following boron treatment (Figure 2). These genes are involved in various pathways, such as pathogen resistance (*subtilisin-like protease SBT1*, *PavSBT1.7*) and lignin biosynthesis (*caffeoylshikimate esterase-like*, *PavCSE.1*) (Meyer et al., 2016; Vanholme et al., 2013), signifying that boron accumulation in cherry fruit reprograms various metabolic pathways. As such, these results imply a diverse role of boron in sweet cherry biology across fruit development. Noteworthy, numerous heat shock proteins (HSPs) were decreased at the S1 stage and subsequently increased in the following stage (S2) in fruit subjected to boron (Figure 2). For example, boron suppressed at S1 the expression of genes encoding Hsp20s, such as *PavHSP20.1*, *PavHSP20.4*, and *PavH SP20.5*, whereas *PavHSP20.2*, *PavHSP20.3*, *PavHSP20.4*, *PavHSP20.6*, and *PavHSP20.7* were induced by boron at S2 (Figure 2F). In parallel, *PavHSP70-1*, *PavHSP70.1*, *PavHSP90A*, and *PavHSP90.1* were downregulated in boron-exposed cherries at S1, while eight genes of Hsp70 and one Hsp90 were upregulated at S2 (Figure 2F), highlighting the contrasting effect of boron in HSPs hallmarks during the early stage of sweet cherry fruit development. However, the knowledge of why and how the differential expression of these HSPs is orchestrated during growth and by the boron treatment deserves to be investigated in the future.

4.3 | Boron can positively or negatively affect several transcription factors during early fruit growth

Another major target of interest in this study was the changes in TFs after the boron treatment. In particular, the altered expression of *PavbHLH25* (bHLH family) and *PavMYB44L* (MYB family) in boron-treated fruit (Figure 3) is indicative of the involvement of boron in the fruit set of self-fertile cherry cultivar via parthenocarp development, since these TFs are associated with parthenocarp in several fruits (Subbaraya et al., 2020). The present study also showed that homeobox-leucine zipper protein ATHB-12-like (*PavATHB.12L*) was decreased in B-exposed cherries at both stages (Figure 3). Given that the *PavATHB.12L* was associated with fruitlet abscission in sweet cherries (Qiu et al., 2020), these findings might be suggestive of boron actions to prevent fruit fall, and, consequently, a likely stimulation of fruit set. Consistent with this, the strong suppression of zinc finger protein ZAT10 TF (*PavZAT10.1*, *.2*) under boron exposure at both stages (Figure 3) may reduce the sensitivity to abscisic acid (Yang et al., 2021), which is linked to the fruitlet abscission in sweet cherry (Qiu et al., 2021), and thereby to fruit set.

4.4 | Key metabolic pathways that are affected by boron across fruit development

Comparative transcriptomic profiling revealed several differences in the expression of numerous boron-responsive genes between the early growth stages examined; such behavior might represent a boron-specific strategy to establish a new developmental dynamic in sweet cherry fruitlet. In this regard, we observed an activation of inositol phosphate metabolism pathway as well as a deactivation of cysteine/methionine metabolism and phenylpropanoid biosynthesis at the S1 stage (Figure 5). In particular, the increased expression of *inositol oxygenase 1* (*PavMIOX*), which convert myo-inositol to glucuronate and is involved in ascorbic acid (AsA) biosynthesis (Munir et al., 2020), suggests that boron may play a role in the formation of antioxidants such as AsA, as an interaction between AsA and boron has already documented (Lukaszewski & Blevins, 1996). In boron-treated fruits at early stage (S1), the lower expression level of *cinnamyl alcohol dehydrogenase* (*PavCAD1*) (Figure 5), which is involved in lignin biosynthesis and catalyzed the final step specific to the production of lignin monomers (Zhang et al., 2017), suggests that boron may have a significant influence on lignin biosynthesis, transposing the hardening of endocarp and forcing a possible late response transition to the hardening stage of the endocarp. In this regard, we also noted that *PavPAL1* and *Pav4CL3* were upregulated in fruit subjected to boron treatment (Figure 6). Although the exact role of PAL in fruit developmental biology remains uncertain, there is evidence indicating that high PAL expression during the early stages of stone fruit formation could be related to an enlargement of all parts of the ovary and lignification of the endocarp (Morelló et al., 2005) and may be correlated to the phenol content upon boron starvation (Camacho-Cristóbal et al., 2002). Furthermore, in fruit exposed to boron, the downregulation of several genes 2C type protein

phosphatase, including *PavPP2C.51*, *PavHAB1* at S1 (Figure 5), is consistent with their known function in fruit ABA perception and signaling (Jia et al., 2013). In parallel, we observed that *serine/threonine-protein kinase* *SAPK1* (*PavSNRK2.7*) was affected by boron at S2 stage. Because *PavSNRK2.7* is an ABA-dependent kinase that regulates plant growth under optimal and stress conditions (Hasan et al., 2022), we anticipate that ABA pathway may be involved in the boron-derived regulation of sweet cherry development (Figure 6).

In higher plants, mature leaves are the primary source of photoassimilates, although other green organs, such as fruit peels, can also participate in carbon accumulation (Yuan et al., 2018). Particularly, the photosynthetic activity of green fruit contributes to fruit growth and this function would appear to be coupled to the induction of gene expression associated with carbon assimilation (Karagiannis et al., 2020). In this work, the abundances of several photosynthetic genes, including *oxygen-evolving enhancer proteins*, *photosystem I and II subunits*, and *chlorophyll a-b binding proteins* as well as of genes involved in protein synthesis, that is, *ribosomes* (60S and 40S *ribosomal proteins*) was induced by boron at the S2 stage (Figure 6), which suggests that the *de novo production* of *photoassimilates* in cherry fruit is enhanced by boron. Since the respiration rate was reduced by boron at the S2 stage (Figure 1C), the overall effect of the induction of photosynthetic genes would be to further increase the carbon use efficiency. Our analysis further revealed activation of carbohydrate metabolism, especially galactose (*PavSIP1.1*, *PavHKL1*, *PavSIP1.2*, *PavPFK3*) and sucrose/trehalose (*PavTPS9.1*, *PavBGLU17*, *PavGH9B1*, *PavCT-BMY*, *PavBAM1*, *PavHKL1*) metabolic pathways in boron-exposed cherries at S2 stage. It was previously shown that stomata on the surface of cherry fruit carry out a real physiological role, contributing to carbon status either directly by assimilating carbon from the atmosphere or through recycling photosynthesis, recapturing the CO₂ liberated by mitochondrial respiration (Vignati et al., 2022). Hence, it is possible that boron may alter photosynthetic carbon assimilation, stomata opening, and sugar metabolism, thus contributing to the initial stages of sweet cherry fruit development, but further physiological research is needed to prove this interaction. Given that, fruit photosynthesis could provide advantages for early fruit growth, as well as maintaining yield, particularly under conditions of stress when leaf photosynthesis may be compromised (Simkin et al., 2020). The effect of boron on the photosynthetic activity of young sweet cherry fruit is worthy of further study.

5 | CONCLUSION

This study reports major developmental events following the preflowering application of boron. The analysis of physiological traits was performed across various fruit developmental stages (S1–S5 stages), revealing that boron application promoted fruit set and induced cell enlargement. We found that primary metabolism induction is a direct response of sweet cherry to boron since an extensive accumulation of several sugars (e.g., fructose, glucose), alcohols (e.g., myo-inositol, maltitol), organic acids (e.g., malic acid, citric acid), amino acids

(e.g., valine, serine) was detected in boron-exposed fruit, especially at early growth period. Genes involved in secondary and amino acid metabolism (i.e., *PavMIOX*, *PavPLPT*, *PavCAD1*) and calcium-binding (i.e., *PavMSS3*, *PavCML31*) appear to be severely affected by boron at the S1 stage. Current results also highlight that sweet cherry fruit response to boron at the S2 stage potentially involves the alternation of genes participating in ribosome biogenesis (e.g., *PavRP53Ae*, *PavRPL2*), sugar homeostasis (e.g., *PavTPS9.2*, *PavBGLU17*), secondary metabolism (e.g., *PavPAL1*, *Pav4CL3*) transport system (*ABC transporters*, e.g., *PavABCG21*, *PavABCG22*) and stomata opening (e.g., *PavIAA9*, *PavIAA11*), underlining the importance of the respective metabolic pathways in sweet cherry developmental programs. Notably, photosynthetic traits appear to be severely affected by boron in developing cherries, particularly at the S2 stage. Various boron-responsive genes were either upregulated (i.e., *PavBAM9*, *PavPIP5K9*) or downregulated (*PavSBT1.7* and *PavCSE.1*) in both stages and may, therefore, globally play important roles in cherries growth. Nevertheless, the present work also characterized several boron-affected HSPs, including *PavbHLH25*, *PavATHB.12L* and *PavZAT10.1*, *.2* that displayed distinct patterns between the examined stages, illustrating that the boron-based HSPs *regulation* occurs with high developmental specificity. To this end, we identified various TFs (*PavbHLH25*, *PavATHB.12 L* and *PavZAT10.1,.2*) affected by boron. Overall, from the observations described here, we propose a schematic draft in which boron influences early fruit growth (Figure 7).

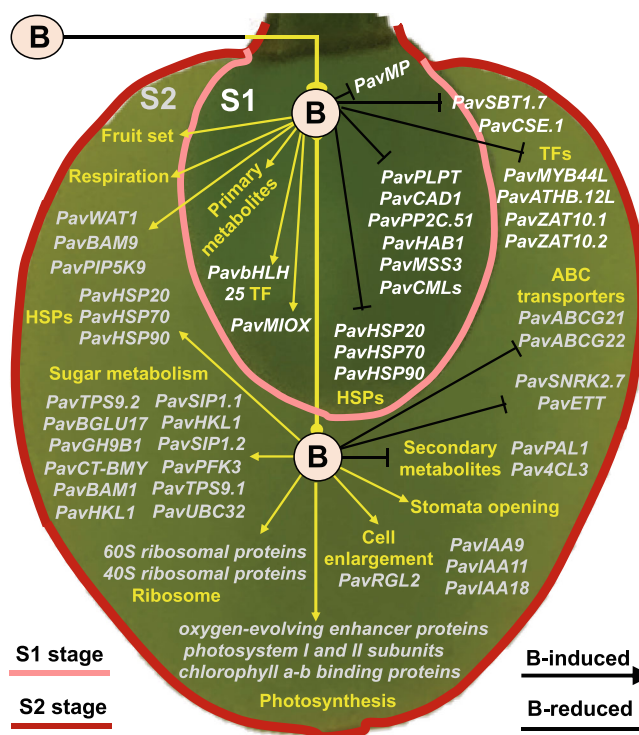


FIGURE 7 A schematic illustration of the key physiological and metabolic changes up- or downregulated by boron in sweet cherry fruit at the S1 and S2 developmental stages. Abbreviations are provided in Table S3.

Further research is required to better understand the role of boron in fruit set and early fruit development in sweet cherry.

AUTHOR CONTRIBUTIONS

Michail Michailidis and Georgia Tanou conceived this study. Michail Michailidis conducted the experiments and wrote the manuscript. Christos Bazakos, Marios Kollaros, Ioannis-Dimosthenis S. Adamakis, Ioannis Ganopoulos and Georgia Tanou conducted the experiments and analyzed data. Athanasios Molassiotis discussed the data and reviewed the initial manuscript. All authors approved the submitted version of the manuscript.

ACKNOWLEDGMENTS

The authors would like to thank Chrysa Krita for her skillful assistance in field sampling and laboratory analysis. The publication of the article in OA mode was financially supported by HEAL-Link.

FUNDING INFORMATION

This work was funded by the Action “Investment Plans of Innovation” of the Operational Program “Central Macedonia 2021-2027”, which is co-funded by the European Regional Development Fund and Greece (Project code: KMP6-0078866).

CONFLICT OF INTEREST STATEMENT

The authors declare no conflict of interest.

DATA AVAILABILITY STATEMENT

The datasets supporting the conclusions of this article are included within the article and its Supplementary material. The Illumina RNA-seq reads are available in NCBI database (Bioproject: PRJNA945231).

ORCID

Athanasios Molassiotis  <https://orcid.org/0000-0001-5118-2244>

Georgia Tanou  <https://orcid.org/0000-0002-9282-2794>

REFERENCES

- Alkio, M., Jonas, U., Declercq, M., van Nocker, S. & Knoche, M. (2014) Transcriptional dynamics of the developing sweet cherry (*Prunus avium* L.) fruit: sequencing, annotation and expression profiling of exocarp-associated genes. *Horticulture Research*, 1, 11. Available from: <https://doi.org/10.1038/hortres.2014.11>
- Beauvoit, B., Belouah, I., Bertin, N., Cakpo, C.B., Colombié, S., Dai, Z. et al. (2018) Putting primary metabolism into perspective to obtain better fruits. *Annals of Botany*, 122, 1–21. Available from: <https://doi.org/10.1093/aob/mcy057>
- Botelho, R.V., Müller, M.M.L., Umburanas, R.C., Laconski, J.M.O. & Terra, M.M. (2022) Boron in fruit crops: plant physiology, deficiency, toxicity, and sources for fertilization. In: *Boron in plants and agriculture: exploring the physiology of boron and its impact on plant growth*. Cambridge, Massachusetts: Academic Press, pp. 29–50.
- Brown, P.H., Bellaloui, N., Wimmer, M.A., Bassil, E.S., Ruiz, J., Hu, H. et al. (2002) Boron in plant biology. *Plant Biology*, 4, 205–223. Available from: <https://doi.org/10.1055/s-2002-25740>
- Camacho-Cristóbal, J.J., Anzellotti, D. & González-Fontes, A. (2002) Changes in phenolic metabolism of tobacco plants during short-term boron deficiency. *Plant Physiology and Biochemistry*, 40, 997–1002. Available from: [https://doi.org/10.1016/S0981-9428\(02\)01463-8](https://doi.org/10.1016/S0981-9428(02)01463-8)
- Canton, M., Drincovich, M.F., Lara, M.V., Vizzotto, G., Walker, R.P., Famiani, F. et al. (2020) Metabolism of stone fruits: reciprocal contribution between primary metabolism and cell wall. *Frontiers in Plant Science*, 11, 1054. Available from: <https://doi.org/10.3389/fpls.2020.01054>
- Carpita, N.C. & Gibeaut, D.M. (1993) Structural models of primary cell walls in flowering plants: consistency of molecular structure with the physical properties of the walls during growth. *The Plant Journal*, 3, 1–30. Available from: <https://doi.org/10.1111/j.1365-313X.1993.tb00007.x>
- David, L.C., Lee, S.K., Bruderer, E., Abt, M.R., Fischer-Stettler, M., Tschopp, M.A. et al. (2022) BETA-AMYLASE9 is a plastidial nonenzymatic regulator of leaf starch degradation. *Plant Physiology*, 188, 191–207. Available from: <https://doi.org/10.1093/plphys/kiab468>
- Fadón, E., Herrero, M. & Rodrigo, J. (2015) Flower development in sweet cherry framed in the BBCH scale. *Scientia Horticulturae (Amsterdam)*, 192, 141–147. Available from: <https://doi.org/10.1016/j.scienta.2015.05.027>
- Falchi, R., Bonghi, C., Drincovich, M.F., Famiani, F., Lara, M.V., Walker, R.P. et al. (2020) Sugar metabolism in stone fruit: source-sink relationships and environmental and agronomical effects. *Frontiers in Plant Science*, 11, 1820. Available from: <https://doi.org/10.3389/fpls.2020.573982>
- Fang, K.F., Du, B.S., Zhang, Q., Xing, Y., Cao, Q.Q. & Qin, L. (2019) Boron deficiency alters cytosolic Ca²⁺ concentration and affects the cell wall components of pollen tubes in *Malus domestica*. *Plant Biology*, 21, 343–351. Available from: <https://doi.org/10.1111/plb.12941>
- García Montiel, F., Serrano, M., Martínez-Romero, D. & Alburquerque, N. (2010) Factors influencing fruit set and quality in different sweet cherry cultivars. *Spanish Journal of Agricultural Research*, 8, 1118. Available from: <https://doi.org/10.5424/sjar/2010084-1238>
- Garratt, M.P.D., O'Connor, R.S., Carvell, C., Fountain, M.T., Breeze, T.D., Pywell, R. et al. (2023) Addressing pollination deficits in orchard crops through habitat management for wild pollinators. *Ecological Applications*, 33, e2743. Available from: <https://doi.org/10.1002/eap.2743>
- Gibeaut, D.M., Whiting, M.D. & Einhorn, T. (2017) Time indices of multiphasic development in genotypes of sweet cherry are similar from dormancy to cessation of pit growth. *Annals of Botany*, 119, 465–475. Available from: <https://doi.org/10.1093/aob/mcw232>
- Goulas, V., Minas, I.S., Kourdoulas, P.M., Lazaridou, A., Molassiotis, A.N., Gerothanassis, I.P. et al. (2015) ¹H NMR metabolic fingerprinting to probe temporal postharvest changes on qualitative attributes and phytochemical profile of sweet cherry fruit. *Frontiers in Plant Science*, 6, 959. Available from: <https://doi.org/10.3389/fpls.2015.00959>
- Hasan, M.M., Liu, X.D., Waseem, M., Guang-Qian, Y., Alabdallah, N.M., Jahan, M.S. et al. (2022) ABA activated SnRK2 kinases: an emerging role in plant growth and physiology. *Plant Signaling & Behavior*, 17, e2071024. Available from: <https://doi.org/10.1080/15592324.2022.2071024>
- Hu, H., Penn, S.G., Lebrilla, C.B. & Brown, P.H. (1997) Isolation and characterization of soluble boron complexes in higher plants: the mechanism of phloem mobility of boron. *Plant Physiology*, 113, 649–655. Available from: <https://doi.org/10.1104/pp.113.2.649>
- Jia, H.F., Lu, D., Sun, J.H., Li, C.L., Xing, Y., Qin, L. et al. (2013) Type 2C protein phosphatase ABI1 is a negative regulator of strawberry fruit ripening. *Journal of Experimental Botany*, 64, 1677–1687. Available from: <https://doi.org/10.1093/jxb/ert028>
- Kappel, F., MacDonald, R., McKenzie, D.L. & Hampson, C. (2003) Sweet cherry improvement at Summerland, Canada. *Acta Horticulturae*, 622, 607–610. Available from: <https://doi.org/10.17660/ActaHortic.2003.622.66>
- Karagiannis, E., Michailidis, M., Tanou, G., Scossa, F., Sarrou, E., Stamatakis, G. et al. (2020) Decoding altitude-activated regulatory mechanisms occurring during apple peel ripening. *Horticulture*

- Research, 7, 120. Available from: <https://doi.org/10.1038/s41438-020-00340-x>
- Langfelder, P. & Horvath, S. (2008) WGCNA: an R package for weighted correlation network analysis. *BMC Bioinformatics*, 9, 559. Available from: <https://doi.org/10.1186/1471-2105-9-559>
- Lisec, J., Schauer, N., Kopka, J., Willmitzer, L. & Fernie, A.R. (2006) Gas chromatography mass spectrometry-based metabolite profiling in plants. *Nature Protocols*, 1, 387–396. Available from: <https://doi.org/10.1038/nprot.2006.59>
- Livak, K.J. & Schmittgen, T.D. (2001) Analysis of relative gene expression data using real-time quantitative PCR and the 2⁻ $\Delta\Delta$ CT method. *Methods*, 25, 402–408. Available from: <https://doi.org/10.1006/meth.2001.1262>
- Lou, Y., Gou, J.Y. & Xue, H.W. (2007) PIP5K9, an *Arabidopsis* phosphatidylinositol monophosphate kinase, interacts with a cytosolic invertase to negatively regulate sugar-mediated root growth. *Plant Cell*, 19, 163–181. Available from: <https://doi.org/10.1105/tpc.106.045658>
- Lukaszewski, K.M. & Blevins, D.G. (1996) Root growth inhibition in boron-deficient or aluminum-stressed squash may be a result of impaired ascorbate metabolism. *Plant Physiology*, 112, 1135–1140. Available from: <https://doi.org/10.1104/pp.112.3.1135>
- Meyer, M., Huttenlocher, F., Cedzich, A., Procopio, S., Stroeder, J., Pau-Roblot, C. et al. (2016) The subtilisin-like protease SBT3 contributes to insect resistance in tomato. *Journal of Experimental Botany*, 67, 4325–4338. Available from: <https://doi.org/10.1093/jxb/erw220>
- Michailidis, M., Karagiannis, E., Bazakos, C., Tanou, G., Ganopoulos, I. & Molassiotis, A. (2021) Genotype- and tissue-specific metabolic networks and hub genes involved in water-induced distinct sweet cherry fruit cracking phenotypes. *Computational and Structural Biotechnology Journal*, 19, 5406–5420. Available from: <https://doi.org/10.1016/j.csbj.2021.09.030>
- Michailidis, M., Karagiannis, E., Tanou, G., Samiotaki, M., Tsiolas, G., Sarrou, E. et al. (2020) Novel insights into the calcium action in cherry fruit development revealed by high-throughput mapping. *Plant Molecular Biology*, 104, 597–614. Available from: <https://doi.org/10.1007/s11103-020-01063-2>
- Morelló, J.R., Romero, M.P., Ramo, T. & Motilva, M.J. (2005) Evaluation of l-phenylalanine ammonia-lyase activity and phenolic profile in olive drupe (*Olea europaea* L.) from fruit setting period to harvesting time. *Plant Science*, 168, 65–72. Available from: <https://doi.org/10.1016/j.plantsci.2004.07.013>
- Munir, S., Mumtaz, M.A., Ahiakpa, J.K., Liu, G., Chen, W., Zhou, G. et al. (2020) Genome-wide analysis of Myo-inositol oxygenase gene family in tomato reveals their involvement in ascorbic acid accumulation. *BMC Genomics*, 21, 1–15. Available from: <https://doi.org/10.1186/s12864-020-6708-8>
- Ogata, H., Goto, S., Sato, K., Fujibuchi, W., Bono, H. & Kanehisa, M. (1999) KEGG: kyoto encyclopedia of genes and genomes. *Nucleic Acids Research*, 27, 29–34. Available from: <https://doi.org/10.1093/nar/27.1.29>
- Pappas, D., Giannoutsou, E., Panteris, E., Gkelis, S. & Adamakis, I.D.S. (2022) Microcystin-LR and cyanobacterial extracts alter the distribution of cell wall matrix components in rice root cells. *Plant Physiology and Biochemistry*, 191, 78–88. Available from: <https://doi.org/10.1016/j.plaphy.2022.09.020>
- Polychroniadou, C., Karagiannis, E., Michailidis, M., Adamakis, I.D.S., Ganopoulos, I., Tanou, G. et al. (2022) Identification of genes and metabolic pathways involved in wounding-induced kiwifruit ripening. *Plant Physiology and Biochemistry*, 179, 179–190. Available from: <https://doi.org/10.1016/j.plaphy.2022.03.027>
- Qiu, Z., Wen, Z., Hou, Q., Qiao, G., Yang, K., Hong, Y. et al. (2021) Cross-talk between transcriptome, phytohormone and HD-ZIP gene family analysis illuminates the molecular mechanism underlying fruitlet abscission in sweet cherry (*Prunus avium* L.). *BMC Plant Biology*, 21, 1–18. Available from: <https://doi.org/10.1186/s12870-021-02940-8>
- Qiu, Z.L., Wen, Z., Yang, K., Tian, T., Qiao, G., Hong, Y. et al. (2020) Comparative proteomics profiling illuminates the fruitlet abscission mechanism of sweet cherry as induced by embryo abortion. *International Journal of Molecular Sciences*, 21, 1200. Available from: <https://doi.org/10.3390/ijms21041200>
- Ranocha, P., Dima, O., Nagy, R., Felten, J., Corratgé-Faillie, C., Novák, O. et al. (2013) Arabidopsis WAT1 is a vacuolar auxin transport facilitator required for auxin homeostasis. *Nature Communications*, 4, 1–9. Available from: <https://doi.org/10.1038/ncomms3625>
- Sabir, I.A., Liu, X., Jiu, S., Whiting, M. & Zhang, C. (2021) Plant growth regulators modify fruit set, fruit quality, and return bloom in sweet cherry. *HortScience*, 56, 922–931. Available from: <https://doi.org/10.21273/hortsci15835-21>
- Schon, M.K. & Blevins, D.G. (1990) Foliar boron applications increase the final number of branches and pods on branches of field-grown soybeans. *Plant Physiology*, 92, 602–607. Available from: <https://doi.org/10.1104/pp.92.3.602>
- Schuster, M. (2017) Self-incompatibility (S) genotypes of cultivated sweet cherries—an overview 2017 (Version 1.0). *OpenAgrar-Repository*, 1–45. Available from: <https://doi.org/10.5073/20171213-111734>
- Sedgley, M. & Griffin, A.R. (1989) *Sexual reproduction of tree crops*. London: Academic Press.
- Shannon, P., Markiel, A., Ozier, O., Baliga, N.S., Wang, J.T., Ramage, D. et al. (2003) Cytoscape: a software environment for integrated models of biomolecular interaction networks. *Genome Research*, 13, 2498–2504. Available from: <https://doi.org/10.1101/gr.1239303>
- Shinozaki, Y., Beauvoit, B.P., Takahara, M., Hao, S., Ezura, K., Andrieu, M.H. et al. (2020) Fruit setting rewires central metabolism via gibberellin cascades. *Proceedings of the National Academy of Sciences of the United States of America*, 117, 23970–23981. Available from: <https://doi.org/10.1073/pnas.2011859117>
- Simkin, A.J., Faralli, M., Ramamoorthy, S. & Lawson, T. (2020) Photosynthesis in non-foliar tissues: implications for yield. *The Plant Journal*, 101, 1001–1015. Available from: <https://doi.org/10.1111/tbj.14633>
- Sotiropoulos, T.E., Molassiotis, A., Almaliotis, D., Moutaridou, G., Dimassi, K., Therios, I. et al. (2006) Growth, nutritional status, chlorophyll content, and antioxidant responses of the apple rootstock MM 111 shoots cultured under high boron concentrations in vitro. *Journal of Plant Nutrition*, 29, 575–583. Available from: <https://doi.org/10.1080/01904160500526956>
- Subbaraya, U., Rajendran, S., Simeon, S., Suthanthiram, B. & Marimuthu Somasundram, S. (2020) Unravelling the regulatory network of transcription factors in parthenocarpy. *Scientia Horticulturae (Amsterdam)*, 261, 108920. Available from: <https://doi.org/10.1016/j.scienta.2019.108920>
- Tanou, G., Minas, I.S., Karagiannis, E., Tsikou, D., Audebert, S., Papadopoulou, K.K. et al. (2015) The impact of sodium nitroprusside and ozone in kiwifruit ripening physiology: a combined gene and protein expression profiling approach. *Annals of Botany*, 116, 649–662. Available from: <https://doi.org/10.1093/aob/mcv107>
- Teribia, N., Tijero, V. & Munné-Bosch, S. (2016) Linking hormonal profiles with variations in sugar and anthocyanin contents during the natural development and ripening of sweet cherries. *New Biotechnology*, 33, 824–833. Available from: <https://doi.org/10.1016/j.nbt.2016.07.015>
- Thomas, P.D., Ebert, D., Muruganujan, A., Mushayama, T., Albou, L.P. & Mi, H. (2022) PANTHER: making genome-scale phylogenetics accessible to all. *Protein Science*, 31, 8–22. Available from: <https://doi.org/10.1002/pro.4218>
- Vanholme, R., Cesarino, I., Rataj, K., Xiao, Y., Sundin, L., Goeminne, G. et al. (2013) Caffeoyl shikimate esterase (CSE) is an enzyme in the lignin biosynthetic pathway in arabidopsis. *Science*, 341, 1103–1106. Available from: <https://doi.org/10.1126/science.1241602>
- Vignati, E., Lipska, M., Dunwell, J.M., Caccamo, M. & Simkin, A.J. (2022) Fruit Development in Sweet Cherry. *Plants*, 11, 1531. Available from: <https://doi.org/10.3390/plants11121531>

- Wang, J., Liu, W., Zhu, D., Hong, P., Zhang, S., Xiao, S. et al. (2020) Chromosome-scale genome assembly of sweet cherry (*Prunus avium* L.) cv. Tieton obtained using long-read and Hi-C sequencing. *Horticulture Research*, 7, 122. Available from: <https://doi.org/10.1038/s41438-020-00343-8>
- Wojcik, P. & Wojcik, M. (2006) Effect of boron fertilization on sweet cherry tree yield and fruit quality. *Journal of Plant Nutrition*, 29, 1755–1766. Available from: <https://doi.org/10.1080/01904160600897471>
- Wojcik, P., Wojcik, M. & Klamkowski, K. (2008) Response of apple trees to boron fertilization under conditions of low soil boron availability. *Scientia Horticulturae (Amsterdam)*, 116, 58–64. Available from: <https://doi.org/10.1016/j.scienta.2007.10.032>
- Yang, K., Li, C.Y., An, J.P., Wang, D.R., Wang, X., Wang, C.K. et al. (2021) The C2H2-type zinc finger transcription factor MdZAT10 negatively regulates drought tolerance in apple. *Plant Physiology and Biochemistry*, 167, 390–399. Available from: <https://doi.org/10.1016/j.plaphy.2021.08.014>
- Yilmaz, A., Mejía-Guerra, M.K., Kurz, K., Liang, X., Welch, L. & Grotewold, E. (2011) AGRIS: the arabidopsis gene regulatory information server, an update. *Nucleic Acids Research*, 39, 1118–1122. Available from: <https://doi.org/10.1093/nar/gkq1120>
- Yuan, Y., Mei, L., Wu, M., Wei, W., Shan, W., Gong, Z. et al. (2018) SIARF10, an auxin response factor, is involved in chlorophyll and sugar accumulation during tomato fruit development. *Journal of Experimental Botany*, 69, 5507–5518. Available from: <https://doi.org/10.1093/jxb/ery328>
- Zhang, X., Zhang, L., Zhang, Q., Xu, J., Liu, W. & Dong, W. (2017) Comparative transcriptome profiling and morphology provide insights into endocarp cleaving of apricot cultivar (*Prunus armeniaca* L.). *BMC Plant Biology*, 17, 1–14. Available from: <https://doi.org/10.1186/s12870-017-1023-5>
- Zhong, R. & Ye, Z.H. (2015) Secondary cell walls: biosynthesis, patterned deposition and transcriptional regulation. *Plant & Cell Physiology*, 56, 195–214. Available from: <https://doi.org/10.1093/pcp/pcu140>
- Ziogas, V., Michailidis, M., Karagiannis, E., Tanou, G. & Molassiotis, A. (2020) Manipulating fruit quality through foliar nutrition In: Amsterdam: Elsevier, pp 401–417. Available from: <https://doi.org/10.1016/b978-0-12-818732-6.00029-0>

SUPPORTING INFORMATION

Additional supporting information can be found online in the Supporting Information section at the end of this article.

How to cite this article: Michailidis, M., Bazakos, C., Kollaros, M., Adamakis, I.-D.S., Ganopoulos, I., Molassiotis, A. et al. (2023) Boron stimulates fruit formation and reprograms developmental metabolism in sweet cherry. *Physiologia Plantarum*, 175(3), e13946. Available from: <https://doi.org/10.1111/ppl.13946>